Iowa State University
Digital Repository

Agricultural and Biosystems Engineering Publications

Agricultural and Biosystems Engineering

2001

Spatial Analysis of NO 3 -N Concentration in Glacial Till

Victor B. Ella
University of the Philippines Los Baños

Stewart W. Melvin
Iowa State University

Rameshwar S. Kanwar
Iowa State University, rskanwar@iastate.edu

Follow this and additional works at: http://lib.dr.iastate.edu/abe_eng_pubs

Part of the Agriculture Commons, Bioresource and Agricultural Engineering Commons, and the Water Resource Management Commons

The complete bibliographic information for this item can be found at http://lib.dr.iastate.edu/abe_eng_pubs/665. For information on how to cite this item, please visit http://lib.dr.iastate.edu/howtocite.html.

This Article is brought to you for free and open access by the Agricultural and Biosystems Engineering at Iowa State University Digital Repository. It has been accepted for inclusion in Agricultural and Biosystems Engineering Publications by an authorized administrator of Iowa State University Digital Repository. For more information, please contact digirep@iastate.edu.

Spatial Analysis of NO 3 -N Concentration in Glacial Till

Abstract

Analysis of the spatial variability of groundwater NO3 –N concentration is a logical step for a meaningful groundwater quality assessment, for mapping out areas of environmental concern, and for developing appropriate management schemes in a glacial till aquitard. This study was conducted to characterize the spatial variability of NO3 –N concentration in shallow (<6.0 m) and deep (>6.0 m) groundwater in a 12–ha. glacial till aquitard and to estimate NO3 –N concentration in unsampled locations. Omnidirectional and directional semivariogram analysis, statistical anisotropy analysis, and model fitting were performed for average and extreme monthly groundwater NO3 –N data. Results indicated a weak spatial structure of NO3 –N concentration for both shallow and deep well data. However, the best–fitted variogram models generally performed satisfactorily during cross validation, yielding a mean reduced error of –0.01 to –0.074 and reduced variance of 0.6 to 2.18. Untransformed shallow–well NO3 –N exhibited a lower range of correlation than deep–well data. Statistical anisotropy was found to coincide with the general groundwater flow directions for the average and maximum observed NO3 –N concentrations in shallow wells. Geostatistical estimation using ordinary kriging indicated relatively higher NO3 –N concentrations at the down–gradient areas for shallow wells and at regions close to nitrogen fertilizer application sites for the deep wells. With satisfactory cross–validation performance of the variogram models, the geostatistical results of this study may be used as basis for estimating spatially variable NO3 –N loading rates in the glacial till aquitard.

Keywords

Spatial variability, Geostatistical analysis, Kriging, Groundwater nitrate–nitrogen, Glacial till

Disciplines

Agriculture | Bioresource and Agricultural Engineering | Water Resource Management

Comments

This article was published in Transactions of the ASAE. Vol. 44(2): 317–327, doi:10.13031/2013.4684. Posted with permission.

This article is available at Iowa State University Digital Repository: http://lib.dr.iastate.edu/abe_eng_pubs/665

SPATIAL ANALYSIS OF NO_3–N CONCENTRATION IN GLACIAL TILL

V. B. Ella, S. W. Melvin, R. S. Kanwar

ABSTRACT. *Analysis of the spatial variability of groundwater NO_3–N concentration is a logical step for a meaningful groundwater quality assessment, for mapping out areas of environmental concern, and for developing appropriate management schemes in a glacial till aquitard. This study was conducted to characterize the spatial variability of NO_3–N concentration in shallow (<6.0 m) and deep (>6.0 m) groundwater in a 12–ha. glacial till aquitard and to estimate NO_3–N concentration in unsampled locations. Omnidirectional and directional semivariogram analysis, statistical anisotropy analysis, and model fitting were performed for average and extreme monthly groundwater NO_3–N data. Results indicated a weak spatial structure of NO_3–N concentration for both shallow and deep well data. However, the best–fitted variogram models generally performed satisfactorily during cross validation, yielding a mean reduced error of –0.01 to –0.074 and reduced variance of 0.6 to 2.18. Untransformed shallow–well NO_3–N exhibited a lower range of correlation than deep–well data. Statistical anisotropy was found to coincide with the general groundwater flow directions for the average and maximum observed NO_3–N concentrations in shallow wells. Geostatistical estimation using ordinary kriging indicated relatively higher NO_3–N concentrations at the down–gradient areas for shallow wells and at regions close to nitrogen fertilizer application sites for the deep wells. With satisfactory cross–validation performance of the variogram models, the geostatistical results of this study may be used as basis for estimating spatially variable NO_3–N loading rates in the glacial till aquitard.*

Keywords. *Spatial variability, Geostatistical analysis, Kriging, Groundwater nitrate–nitrogen, Glacial till.*

Nitrate–nitrogen (NO_3–N) concentrations in groundwater observed in glacial till and other geologic units vary in space and time due to spatially varying soil and hydrologic conditions along with spatial variations in nitrogen fertilizer application. The characterization of spatial variability is a logical step not only in attempting to generate a meaningful assessment of groundwater quality in terms of nitrate but more importantly for mapping out areas of environmental concern and for developing appropriate management and remediation schemes. An analysis of its spatial structure could also serve as basis for determining recommendable groundwater sampling strategies in terms of spacing. Moreover, spatial variability analysis of NO_3–N concentrations could serve as a basis for estimating NO_3–N loading rates.

Geostatistical methods rank among the most fundamentally sound techniques for characterizing spatial variability of such groundwater quality indicators as NO_3–N concentrations. Unlike classical statistical methods, which are mainly concerned with examining the statistical distribution, geostatistics take into account the interpretation of not only the statistical distribution but also the spatial relationships or correlation between the sample data. These techniques deviate from classical statistics in that they are not linked to a population distribution model that assumes the samples to be normally distributed and uncorrelated. Considering the spatially correlated nature of hydrogeologic data, problems associated with spatial characterization and estimation of such data could be addressed more effectively by geostatistical methods. From a practical standpoint, this technique can also be employed even for sparse, often biased, and often expensive sample data (Rouhani et al., 1996). It is a down–to–earth approach and hence well accepted among practitioners (Kitanidis, 1997).

Although a number of studies on geostatistical analysis of NO_3–N have been reported (e.g., Espinosa et al., 1996; Goderya et al., 1996), no study on the geostatistical analysis of NO_3–N concentration in glacial till in Iowa has been published. Hence, this study was conducted to fill this gap. Specifically, the objectives of this study are: 1) to characterize the spatial behavior of NO_3–N concentrations in groundwater observed in both shallow and deep wells installed in glacial till, and 2) to perform geostatistical estimation of NO_3–N concentrations in unsampled locations using kriging techniques.

THEORETICAL BACKGROUND

The most essential theoretical ideas involved in geostatistical analysis and estimation are briefly reviewed in this section. A more thorough and extensive discussion on geostatistics can be found in Journel and Huibregdts (1978), Isaaks and Srivastava (1989), Clark (1979), and Kitanidis (1997), among others.

The heart of geostatistical techniques is the analysis of the spatial structure of the variable of interest through variogram

Article was submitted for review in September 1999; approved for publication by the Soil & Water Division of ASAE in October 2000. Presented at the 1999 ASAE Annual Meeting as Paper No. 99–2004.

Journal paper No. J–18571 of the Iowa Agriculture and Home Economics Experiment Station, Ames, Iowa. Project No. 3415 and supported by Hatch Act and State of Iowa funds.

The authors are **Victor B. Ella,** Associate Professor and Chair, Land and Water Resources Division, Institute of Agricultural Engineering, University of the Philippines at Los Banos, former Graduate Research Assistant, Agricultural and Biosystems Engineering Department, Iowa State University, Ames, Iowa; **Stewart W. Melvin,** ***ASAE Fellow Engineer***, Professor and Head; and **Rameshwar S. Kanwar,** ***ASAE Member Engineer***, Professor, Agricultural and Biosystems Engineering Department, Iowa State University, Ames, Iowa. **Corresponding author**: Victor B. Ella, Land and Water Resources Division, Institute of Agricultural Engineering, University of the Philippines at Los Banos, Laguna 4031, Philippines; phone: 63–49–536–2387; fax: 63–49–536–2387; e–mail: vella@iastate.edu or victor.ella@up.edu.ph.

© 2001 American Society of Agricultural Engineers

analysis. A variogram is a plot of the average squared differences between the data values as a function of the separation distance and is commonly defined by:

$$\gamma(h,\alpha)=\frac{1}{2N(h,\alpha)}\sum_{i=1}^{N}\left[z(x_i)-z(x_i+h)\right]^2 \tag{1}$$

where

$\gamma(h,\alpha)$ = semivariance, which is a function of both the magnitude of the lag distance (h) and its direction (α)

N = number of pair of values

$z(x_i)$ = random variable at location x_i.

Equation 1 is based on an intrinsic assumption that the variance of the increment $[z(x_i) - z(x_i + h)]$ is finite and does not depend on x_i for any vector. This is in addition to the other required condition for second–order stationarity of a random function, which is that the expected value $E\{z(x_i)\}$ exists and does not depend on the position x_i (Journel and Huijbregts, 1978; and Isaaks and Srivastava, 1989).

Semivariogram analysis is often obscured by the presence of outliers for most environmental data. This problem can be solved either by performing the traditional exploratory data analysis or by applying a robust estimator. For most hydrogeologic applications, the former is often a practicable approach and is recommended in recent literature (Kitanidis, 1997).

One of the basic requirements for the choice of variogram model is for the function to satisfy a mathematical condition known as positive definiteness (Isaaks and Srivastava, 1989). This is to ensure that the kriging equations will have one, and only one, stable solution. For most practical applications, variograms are modeled using functions that are known to be positive definite, such as spherical, Gaussian, or exponential functions, or a combination of them.

To objectively evaluate the cross–validation results, a number of statistical criteria have been proposed (e.g., Gambolati and Volpi, 1979; Isaaks and Srivastava, 1989; and Kitanidis, 1997). These criteria include: 1) kriged average error (KAE), 2) kriged reduced mean square error (KRMSE), 3) kriged mean square error (KMSE), reduced mean (RM), and reduced variance (RV).

The kriged average error (KAE) is used as a criterion for testing the degree of systematic error present and is calculated as:

$$KAE=\frac{1}{N}\sum_{i=1}^{N}\left(z_i-z_i^*\right) \tag{2}$$

where

z_i = actual value at location i

z^*_i = kriged estimate at location i

N = number of pairs of actual and estimated values.

The KAE value should be as close to zero as possible.

The accuracy of estimation is tested by the kriged mean square error (KMSE), which is calculated as:

$$KMSE=\left(\frac{1}{N}\sum_{i=1}^{N}\left(z_i-z_i^*\right)^2\right)^{1/2} \tag{3}$$

This value should be less than the variance of the actual values.

The kriged reduced mean square error (KRMSE) is used to check the consistency between the estimation errors and the standard deviation of the actual values. This is calculated as:

$$KRMSE=\left(\frac{1}{N}\sum_{i=1}^{N}\left[\frac{\left(z_i-z_i^*\right)}{s}\right]^2\right)^{1/2} \tag{4}$$

where s = standard deviation of actual values; the other terms are as previously defined. This value should be within the range $1 \pm [2(2/N)^{1/2}]$ for the model to be acceptable.

Yates and Yates (1990) and Kitanidis (1997), among others, recommend using the normalized residuals, as in the case of KRMSE. The two basic criteria used are generally called the reduced mean (RM) and the reduced variance (RV). These are calculated respectively as:

$$RM=\frac{1}{N}\sum_{i=1}^{N}\left[\frac{\left(z_i-z_i^*\right)}{s}\right] \tag{5}$$

and

$$RV=\frac{1}{N}\sum_{i=1}^{N}\left[\frac{\left(z_i-z_i^*\right)}{s}\right]^2 \tag{6}$$

The reduced mean and reduced variance should be close to zero and one, respectively, for the model to be acceptable.

Geostatistical estimation may consequently be accomplished through kriging using the cross–validated variograms. Kriging is a weighted moving average, which under the intrinsic assumption has an estimator of the form:

$$Z^*(x_0)=\sum_{i=1}^{N}w_i Z(x_i) \tag{7}$$

where

N = number of measured values $Z(x_i)$ involved in the estimation of the unrecorded point x_0

w_i = weighting factor.

The problem, therefore, revolves around the determination of the weights w_i such that the estimator $Z^*(x_0)$ is unbiased. Hence:

$$E\left\{Z^*(x_0)-Z(x_0)\right\}=0 \tag{8}$$

and

$$\sigma_k^2(x_0)=\mathrm{Var}\left\{Z^*(x_0)-Z(x_0)\right\}=\text{minimum} \tag{9}$$

The condition for minimum variance expressed in equation 9 subject to

$$\sum_{i=1}^{N}w_i=1$$

can be shown in terms of the covariance C to be:

$$\sigma_k^2(x_0) = \sum_i \sum_j w_i w_j C(x_i, x_j) + C(0) - 2\sum_i w_i C(x_i, x_0) \qquad (10)$$

In terms of semivariogram, equation 10 becomes:

$$\sigma_k^2(x_0) = -\sum_i \sum_j w_i w_j \gamma(x_i, x_j) + 2\sum_i w_i \gamma(x_i, x_0) \qquad (11)$$

where $\gamma(x_i,x_j)$ represents a vector with origin at x_i and extremity at x_j.

Equation 11 is minimized subject to the constraint

$$\sum_{i=1}^{N} w_i = 1$$

This minimization involves Lagrangian techniques in which all the partial N derivatives are set to zero. The kriging system is thus obtained as:

$$\sum_{j=1}^{N} w_j \gamma(x_i, x_j) + \mu = \gamma(x_i, x_0), \text{ i= 1 to N} \qquad (12)$$

$$\sum_{j=1}^{N} w_j = 1$$

where μ = Lagrangian multiplier.

Solution to the above system of equations yields N weights w_j and one Lagrangian multiplier, making it possible to estimate the value of $Z^*(x_0)$ and its corresponding estimation variance.

Site Description and Experimental Methods

The spatial groundwater NO_3–N concentration data used in this study were gathered at the 12–ha field site at Iowa State University's Agricultural Engineering and Agronomy Research Center located 11 km west of Ames, Iowa (fig. 1). The site is situated in the Des Moines lobe of Wisconsin–age till, the most recent glaciated region in Iowa. The uppermost layer consists of Nicollet loam soil. Well logging previously conducted at the site indicated the presence of loess and weathered till to a depth of 3.7 m and unweathered till extending to a depth of 18.6 m (Kanwar et al., 1993). The average stratigraphy of the site is shown in table 1.

The site has a general land slope of less than 2% and an existing subsurface drainage system. The area consists of several experimental plots where either continuous corn or corn–soybean rotation has been practiced. Nitrogen fertilizer and livestock manure have been applied to these plots as part of research efforts to determine appropriate agricultural management practices among other objectives.

A total of 23 shallow (<6.0 m) and 19 deep (>6.0 m) wells constructed in 1989 at the site were used in this study. Although the average depth of the weathered till is 3.7 m, a cutoff of 6.0 m was used to arbitrarily distinguish between shallow and deep groundwater to ensure greater sampling size for geostatistical analysis. Moreover, most of the 6 m wells are screened within the weathered till layer. Hence, each well classification extracts groundwater from a practically homogeneous hydrogeologic unit. Figure 2 shows the spatial distribution of the various wells, which are clustered at 8 different locations. Well sites 1, 3, and 5 are located at the site periphery, while well sites 2, 6, 7, and 8 are located at the inner portion of the field. The wells at site 4 were not considered in this study because these wells are screened below the unweathered till layer (24 to 84 m deep) and no NO_3–N data exist for these wells. The spatial

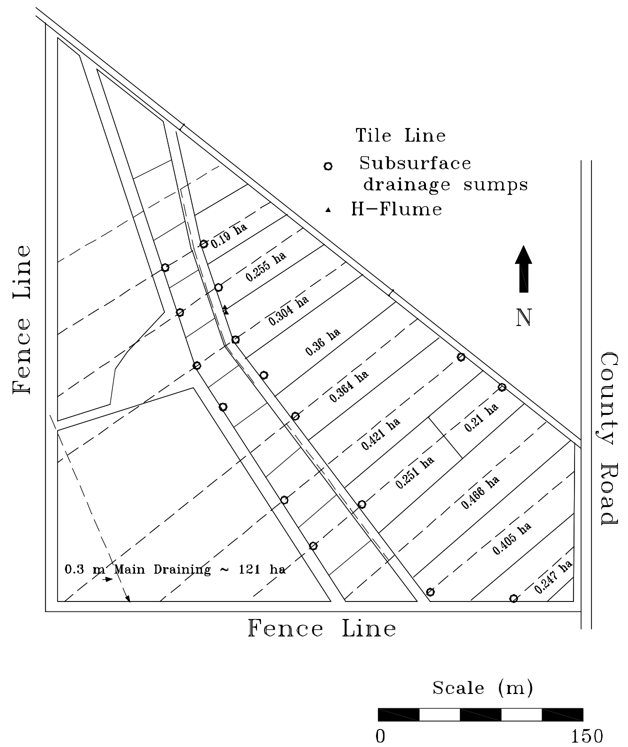

Figure 1. Site map of Iowa State University's Agricultural Engineering and Agronomy Research Center.

Table 1. Average stratigraphy at the glacial till research site.

Depth (m) From	Depth (m) To	Thickness (m)	Description
0	0.6	0.6	Soil zone
0.6	3.7	3.1	Weathered Wisconsin–age till
3.7	22.3	18.6	Unweathered Wisconsin–age till
22.3	25.3	3.0	Loess
25.3	30.5	5.2	Paleosol
30.5	48.2	17.7	Pre–Illinoian weathered till
48.2	72.2	24.0	Pre–Illinoian unweathered till
72.2	79.3	7.1	Rubble zone, boulders, till
79.3	89.9	10.6	Unweathered till, wood pieces, gravel
89.9	101.2	11.3	Sandy till and reworked shale
101.2	103.6	2.4	Sandstone
103.6	109.7	6.1	Shale with sandstone layers
109.7	128.3	18.6	Layers of sandstone, siltstone, slate, and shale

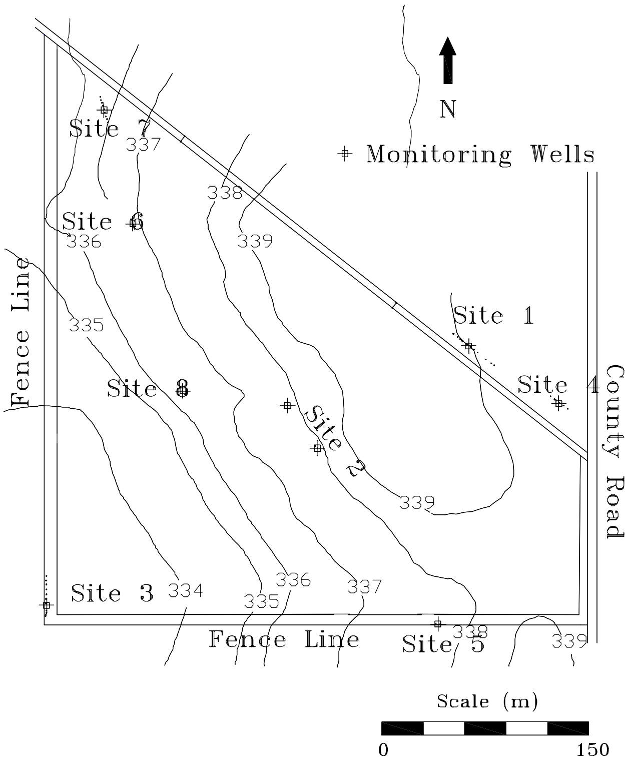

Site 1: 3 shallow wells; 5 deep wells
Site 2: 2 shallow wells; 4 deep wells
Site 3: 3 shallow wells; 5 deep wells
Site 4: 5 deep wells
Site 5: 2 shallow wells; 1 deep well
Site 6: 2 shallow wells; 1 deep well
Site 7: 9 shallow wells; 1 deepwell
Site 8: 2 shallow wells; 1 deep well

Figure 2. Layout of the various monitoring wells and topography at the research site.

coordinates used were obtained from the surveying results performed by Kanwar et al. (1993).

Groundwater samples were collected on a monthly basis for shallow wells and on bimonthly basis for deep wells. The wells were purged a day prior to sampling to obtain samples representative of the formation. Purging and sampling were performed using either a hand pump or a peristaltic pump. The collected samples were analyzed for NO_3–N content at the National Soil Tilth Laboratory, USDA, Ames, Iowa, using a Lachat flow injection autoanalyzer with a detection limit of 1.0 mg/L.

METHODOLOGY FOR GEOSTATISTICAL ANALYSIS

To maintain data homogeneity and to obtain adequate sampling size for geostatistical analysis, the observed data were grouped into two sets: shallow–well groundwater NO_3–N (<6.0 m) and deep–well groundwater NO_3–N (6.0 to 20.0 m). Geostatistical analysis was performed for each data set. Data on NO_3–N concentrations over the most recent years (1994 to 1999) were assembled and the average, minimum, and maximum monthly observed values were chosen for the analysis.

Exploratory data analysis was performed prior to geostatistical analysis to check for any outliers in the data set. A test for normality was similarly performed using the Kolmogorov–Smirnov test to determine whether or not data transformation was necessary.

Omnidirectional semivariograms were then generated using the geostatistical program GEOPACK (Yates and Yates, 1990) to determine the existence of spatial continuity in each layer. Directional semivariograms were subsequently generated to determine any possible statistical anisotropy. Several trial tolerance angles were used, and the resulting variogram pairs were assessed for adequacy. The smallest tolerance angle that produced an adequate number of pairs was chosen. Theoretical semivariograms were then fitted to the experimental semivariograms using a nonlinear least squares minimization technique developed by Marquardt (1963). The various variogram parameters, such as the range, sill, and nugget effect, were then determined for both the mean isotropic and anisotropic variogram models.

In all cases, cross validation was performed using another geostatistical analysis program, GEO–EAS (Englund and Sparks, 1991), linked to GEOPACK. The objective was to check the accuracy and acceptability of the chosen variogram models and to determine a basis for choosing the best models for geostatistical estimation purposes. The cross–validation procedure used employs a "jack–knifing" approach, which involves kriging estimation of the value of the random function of interest at every known sampling location but excluding the known value from the estimation process. Model accuracy and consistency of errors were then assessed using various cross–validation criteria, such as mean reduced error (MRE), reduced variance (RV), kriged average error (KAE), kriged mean square error (KMSE), and kriged reduced mean square error (KRMSE).

Ordinary kriging was then carried out using GEOPACK and employing the variogram models that yielded the best cross–validation results to produce estimates of NO_3–N concentrations at unsampled locations and to visually capture the most probable spatial variability of NO_3–N concentrations at the site.

RESULTS AND DISCUSSION

EXPLORATORY DATA ANALYSIS AND DATA SELECTION

Preliminary univariate statistical analysis for the average NO_3–N concentrations in each well from 1994 to 1999 indicated a range of 0.0 to 16.5 mg/L for shallow wells (< 6.0 m) and 0.0 to 2.3 mg/L for deep wells (6.0 to 20.0 m). The sampling dates for each year generally covered the period from May to October. The monthly field average NO_3–N concentration in the shallow wells ranged from 1.4 mg/L in May 1994 to 5.7 mg/L in August 1994. However, the latter value was based on limited groundwater samples; hence, the next largest field average NO_3–N concentration, 3.7 mg/L observed in June 1998, was considered to be more representative of the extreme condition. The observed NO_3–N data for May 1994 and June 1998 were consequently used to represent minimum and maximum conditions for shallow groundwater NO_3–N concentrations at the site. For deep–well data, on the other hand, the sets with extreme areal averages proved to be inadequate for spatial analytical purposes since the NO_3–N concentrations observed in deep groundwater were generally zero for the period considered. Hence, only the average values for the deep–well NO_3–N concentrations were considered in this study.

Table 2 shows the univariate statistics for the average NO_3–N concentration in shallow and deep wells. The NO_3–N concentration averaged 2.3 and 0.2 mg/L for the shallow and deep groundwater, respectively. The relatively high standard deviation of 4.6 mg/L for the shallow–well data may be attributed to the relatively high NO_3–N concentrations in shallow wells 3–A, 5–A, and 5–B. However, these values were not considered as outliers because observed NO_3–N concentrations in these wells throughout the 6–year period consistently showed practically the same order of magnitude. For deep wells, the NO_3–N data observed in well 2–60S were not considered as outliers since historical trends similarly justified the inclusion of this well in the analysis. While these seemingly outlying data values were retained, data observed in well 3–I were discarded because this well is screened through both the weathered and unweathered till and hence allows the entry of NO_3–N from both shallow and deep groundwater.

Both shallow and deep well NO_3–N data exhibited positive skewness. A test for normality using the Kolmogorov–Smirnov test at 5% significance level proved that the chosen data sets for shallow and deep wells are not normally distributed, as shown in table 3. Data transformation using the square root for the shallow–well data and the fourth root for the deep–well data proved to be adequate to normalize the values based on the Kolmogorov–Smirnov test.

Table 2. Univariate statistics for average NO_3–N concentration in shallow and deep wells.

Statistic	Shallow Wells (< 6.0 m)	Deep Wells[a] (6.0 – 20.0 m)
Number of observations	23	18
Mean (mg/L)	2.3	0.2
Standard deviation (mg/L)	4.6	0.5
Skewness	2.0	3.5
Minimum (mg/L)	0.0	0.0
Median (mg/L)	0.1	0.0
Maximum (mg/L)	16.5	2.3

[a] Excludes well 3–I.

Table 3. Results of Kolmogorov–Smirnov test for normality of NO_3–N concentration.

	N	Dstat	Dcrit[a]	Conclusion
Shallow wells				
Average	23	0.32	0.28	Data are not normally distributed
Maximum	18	0.32	0.31	Data are not normally distributed
Minimum	23	0.47	0.28	Data are not normally distributed
Deep wells				
Average	18	0.42	0.38	Data are not normally distributed

[a] At 5% level of significance.

Variogram Analysis

Omnidirectional semivariograms were generated for the selected NO_3–N concentration data to analyze the occurrence of spatial continuity. A lag spacing equal to the average spacing between neighbors and a lag tolerance equal to half the lag spacing were used, as suggested by Isaaks and Srivastava (1989). The semivariances generally increased with increasing separation distances. The semivariogram for the average values in shallow wells yielded a relatively well–defined trend up to a lag distance of 100 m, beyond which the spatial structure became erratic, as shown in figure 3. The presence of a nugget effect is also apparent in this semivariogram, indicating the presence of short–scale variations occurring at a scale smaller than the closest sample spacing. In fact, examination of raw data indicates that NO_3–N concentrations could vary largely within very short spacing. For instance, wells 3–A and 3–B, spaced about 3.5 m apart, have average NO_3–N concentration values of 16.5 and 1.7 mg/L, respectively.

In the case of NO_3–N values for the minimum and maximum observed conditions, the semivariograms exhibited poor spatial structure (figs. 4 and 5) and greater erratic behavior than did the average observed condition. Both short– and large–scale variations exist in the semivariograms, as demonstrated by the presence of extreme semivariance values at both small and large separation distances.

The semivariogram for the average NO_3–N values observed in deep wells similarly exhibited a poor spatial structure, particularly at high lag distances. Both short– and large–scale variations are also evident from the generated semivariogram (fig. 6). It is also apparent from the variogram analysis that the range of correlation for the untransformed shallow groundwater NO_3–N appears to be shorter than that for the deep groundwater NO_3–N. This implies that a relatively shorter groundwater sampling spacing may be required for shallow–well NO_3–N detection.

Anisotropy Analysis

To determine the presence of preferential directions of spatial continuity, six directional semivariograms for the shallow–well data were generated at 0, 30, 60, 90, 120 and 150 degrees relative to the easting direction. A trial–and–error approach indicated that a tolerance angle of 30 degrees

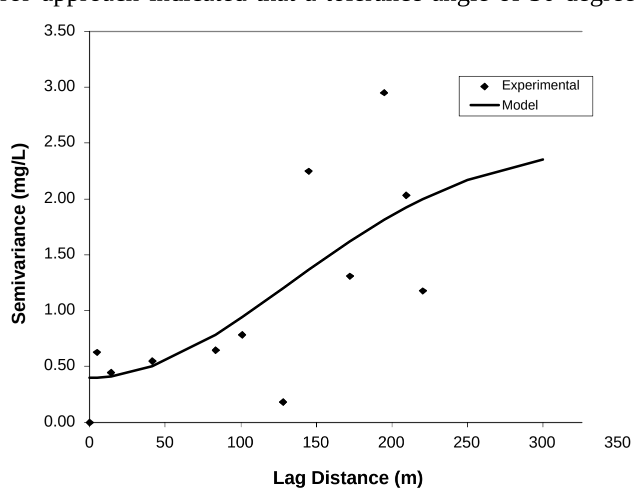

Figure 3. Omnidirectional semivariogram of the square root of NO_3–N concentration in shallow wells using average values.

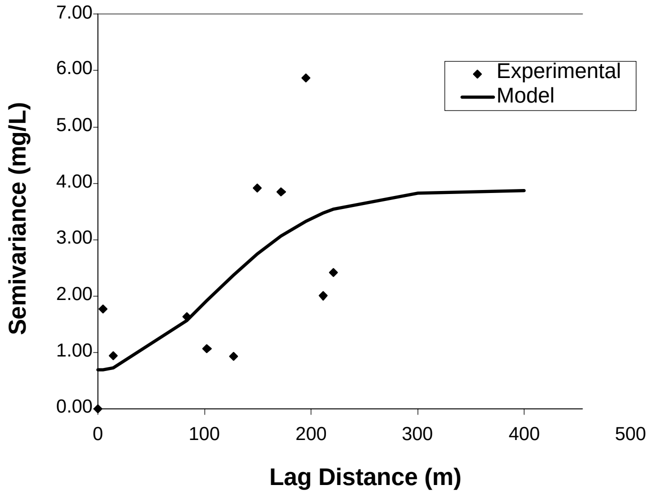

Figure 4. Omnidirectional semivariogram for the square root of NO_3–N concentration in shallow wells using maximum observed values.

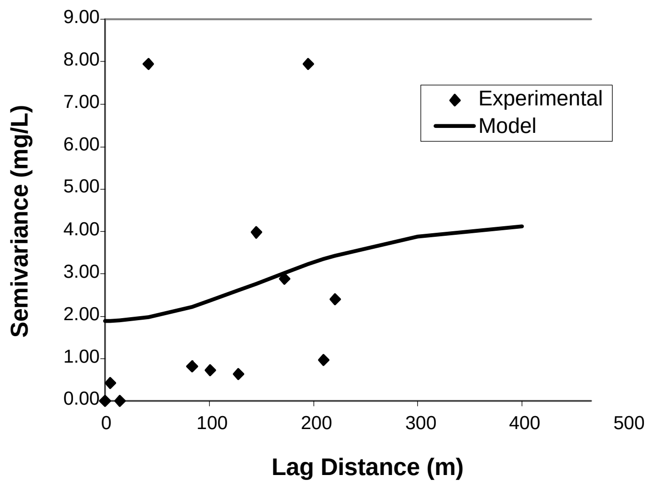

Figure 5. Omnidirectional semivariogram for square root of NO_3–N concentration in shallow wells using minimum observed values.

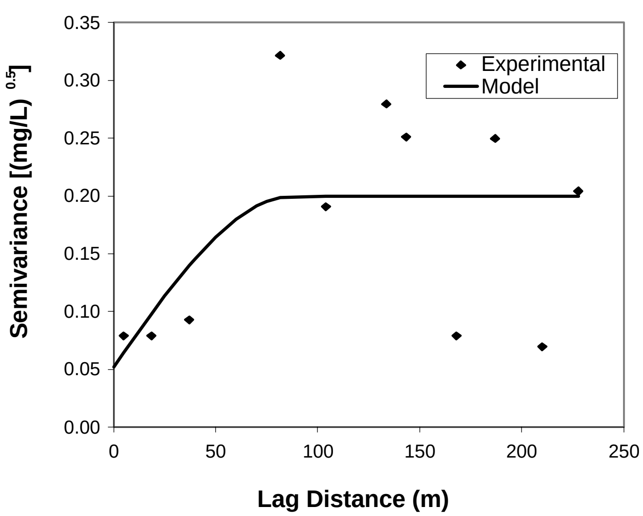

Figure 6. Omnidirectional semivariogram for the fourth root of NO_3–N concentration in deep wells using average observed values.

was adequate for this purpose. The ranges, sills, and nugget effects of the directional semivariograms are shown in table 4. Orthogonal analysis indicates the presence of anisotropy along the 30–degree direction with an approximate anisotropy ratio of 5.0. A rough examination of the topographic and hydrologic conditions at the site appears to logically fit this statistical phenomenon, i.e., greater spatial continuity in this direction approximately coincides with the general groundwater flow and downhill directions. The directional semivariograms for the deep–well NO_3–N data, on the other hand, proved to be too erratic to determine reasonable values for the range, sill, and nugget effect. Hence, anisotropy analysis was not pursued for this data set.

Model Fitting

Despite the lack of well–defined spatial continuity of the semivariograms, models based on positive definite functions fitted satisfactorily with experimental results. For the shallow–well data, a Gaussian model provided a generally good fit, while a spherical model reasonably captured the general trend of the variogram for the deep–well data (figs. 3 to 6). The fitted theoretical models used for the shallow– and deep–well data sets under average conditions are given in table 5.

Table 4. Directional semivariogram model parameters for the untransformed and transformed NO_3–N concentration for shallow and deep wells.

	Range (m)	Sill–nugget	Nugget Effect
Shallow well data			
Average			
Untransformed	202.0	45.3	0.0
Square root	185.2	2.1	0.4
Maximum			
Untransformed	180.1	65.4	6.5
Square root	146.7	3.2	0.7
Minimum			
Untransformed	203.4	28.6	28.4
Square root	207.5	2.3	1.9
Deep well data			
Average			
Untransformed	417.00	0.40	0.030
Fourth root	88.11	0.15	0.052

Table 5. Fitted semivariogram models for the transformed NO_3–N concentrations in shallow and deep wells using average values.

	Fitted Model
Shallow well	$\gamma(h) = 0.4 + 2.11\left[1 - e^{\left(-3h^2\right)/18522}\right]$
Deep well	$\gamma(h) = 0.052 + 0.15\left[\frac{3}{2}\left(\frac{h}{88.1}\right) - \frac{1}{2}\left(\frac{h}{88.1}\right)^3\right]$ for $h \le 88.1$
	$\gamma(h) = 0.202$ for $h > 88.1$

Cross Validation

The acceptability of the chosen variogram models was tested through cross validation using various statistical criteria. While all variogram models yielded satisfactory validation results, the anisotropic Gaussian models for the average and maximum observed NO_3–N concentration and the isotropic Gaussian model for the minimum condition in shallow wells provided the best validation results. As shown in table 6, these models yielded kriged average errors (KAE) and mean reduced errors (MRE) closer to 0, kriged mean square errors (KMSE) less than the variance of observed data, reduced variances (RV) close to 1.0, and a kriged reduced mean square error (KRMSE) falling within the expected range of $1 \pm [2(2/n)^{1/2}]$. The lone model for the average NO_3–N concentration in deep wells similarly performed satisfactorily during cross validation, as all parameters fell within the expected values of the validation criteria with the exception of the KMSE criterion. For rough estimation purposes, however, the selected model may be considered to be adequate.

Kriging Estimation and Interpretation of Spatial Distribution

The variogram models that yielded the best cross–validation results were used in the estimation of shallow and deep groundwater NO_3–N concentration at unsampled locations using ordinary kriging. The kriged values were backtransformed and plotted to form contour maps to visually capture the spatial distribution of groundwater NO_3–N concentrations in the geologic unit under average, minimum, and maximum observed conditions.

Figures 7 and 8 show the contour maps of the backtransformed NO_3–N concentrations using the average and maximum observed values for shallow wells. It is apparent from the contour maps that greater NO_3–N concentrations in shallow wells prevail at areas close to well sites 3 and 5. These sites occur at low–lying areas and hence are often subjected to runoff containing NO_3–N, which emanates from the experimental field plots located at the central portion of the site and from the neighboring farms. This leads to eventual surface detention and subsurface leaching during high rainfall periods at these depressed areas. These high NO_3–N concentration sites also occur at areas with relatively low piezometric head, indicating the potential contribution of groundwater movement to the spatial variability of NO_3–N concentration. These are all further depicted in figure 9, which shows an overlay of the surface elevation, groundwater elevation, and average NO_3–N concentration.

Despite the weak spatial structure of NO_3–N concentration in glacial till, the geostatistically estimated NO_3–N concentrations generated in this study may prove useful for estimating spatially variable NO_3–N loading rates owing to satisfactory cross–validation results of the variogram models used. The NO_3–N loading rate is a function of groundwater recharge and NO_3–N concentration in groundwater. Hence, the results of this study may be used for this purpose and may even be extended for analyzing the spatial variability of NO_3–N loading rates. Furthermore, the results may serve as basis for developing appropriate agricultural management schemes to minimize the concentration of NO_3–N in certain areas of the glacial till aquitard.

The contour map of the backtransformed average NO_3–N concentration for the deep wells (fig. 10) also exhibited greater concentrations of NO_3–N at the nitrogen fertilizer application areas. While the insufficiency of data may not fully confirm this trend, this spatial distribution may be possibly due to the fact that deeper leaching of NO_3–N is likely to occur to a larger extent in the vicinity of N–fertilizer application areas than in other areas. Although rainfall runoff would significantly reduce the sources of NO_3–N for further leaching within the application areas, there would still be sufficient residual NO_3–N in these areas to cause deeper leaching in the long run. Furthermore, the low hydraulic conductivity of the deeper layers greatly reduces the movement of NO_3–N towards the down–gradient directions. Nevertheless, further investigation of the spatial variability of NO_3–N in deep groundwater using more extensive data sets may be necessary to obtain more conclusive findings.

Table 6. Cross validation results.

			Cross Validation Criteria			
	Semivariogram Model	KAE	KMSE	KRMSE	MRE	RV
Shallow Wells						
Average	Mean isotropic model	–0.0174	1.1	1.41	–0.027	1.98
	Anisotropic model	–0.0103	1.05	1.35	–0.015	1.83
	Expected value	0.00	< 1.61	–0.41 to 1.6	0.0	1.00
Maximum	Mean isotropic model	–0.072	1.55	1.49	–0.02	2.22
	Anisotropic model	–0.053	1.55	1.48	–0.01	2.18
	Expected value	0.00	< 2.63	–0.33 to 1.67	0.0	1.00
Minimum	Mean isotropic model	0.00094	1.29	0.77	–0.0011	0.598
	Anisotropic model	–0.057	1.24	0.73	–0.028	0.539
	Expected value	0.00	< 1.27	–0.4 to 1.6	0.0	1.00
Deep Wells						
	Mean isotropic model	0.054	0.417	1.18	0.074	1.395
	Expected value	0.00	< 0.139	0.27 to 1.73	0.0	1.00

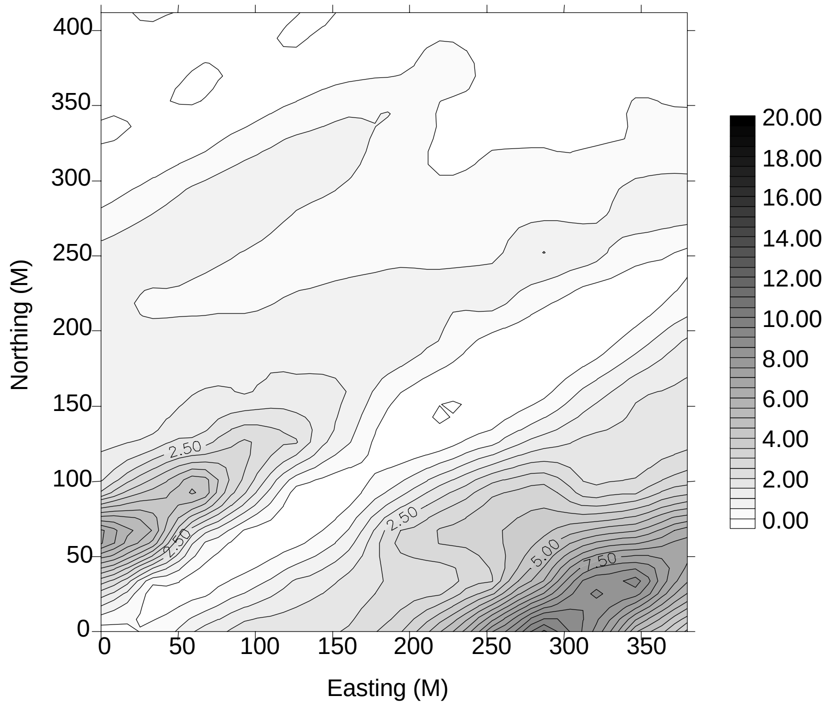

Figure 7. Contour map of backtransformed kriged estimates of NO_3–N concentration in shallow groundwater using average observed values (NO_3–N in mg/L).

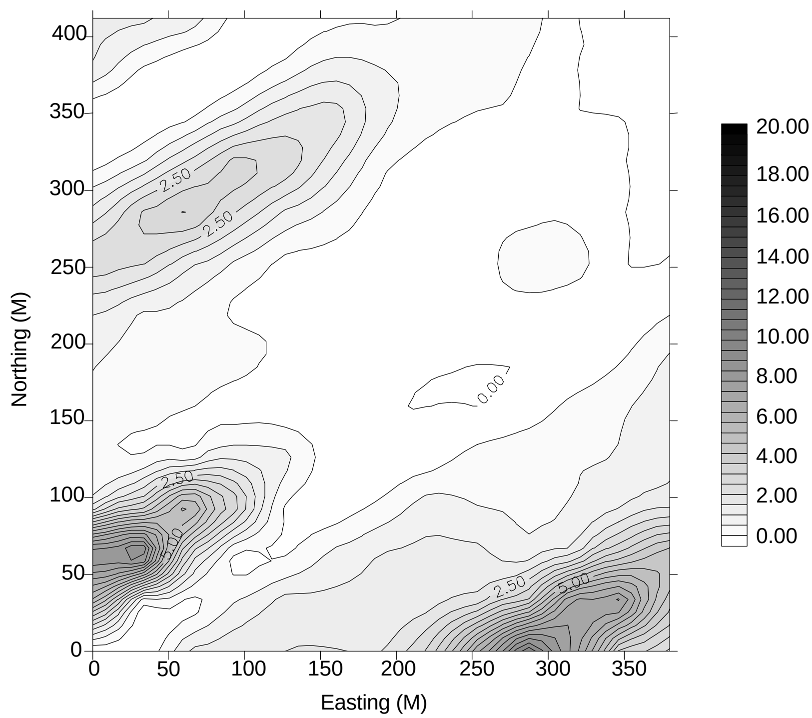

Figure 8. Contour map of backtransformed kriged estimates of NO_3–N concentration in shallow groundwater using maximum observed values (NO_3–N in mg/L).

CONCLUSIONS

The geostatistical analysis of NO_3–N concentration in both shallow and deep groundwater performed in this study generated useful information about the spatial behavior of this groundwater quality indicator in the glacial till aquitard. The average and extreme NO_3–N concentrations observed in shallow and deep wells in the glacial till aquitard exhibited a relatively weak spatial structure due to the presence of both short– and large–scale variations. This may be partly attributed to the spatial variability of soil and hydrogeologic conditions that govern the movement and transformation of nitrates in groundwater.

The average and maximum NO_3–N concentrations observed in shallow groundwater exhibited statistical anisotropy coinciding with the general groundwater flow and downsloping directions, indicating the large influence of both surface runoff and groundwater movement in the spatial distribution of groundwater NO_3–N. On the basis of geostatistical estimation results, higher NO_3–N concentrations were observed in low–lying and down–gradient areas than in other areas for shallow groundwater.

Conversely, the average NO_3–N concentrations for deep groundwater were greater in areas directly underneath the NO_3–N source loading areas than elsewhere. These results indicate that the influence of surface runoff and groundwater movement in the transport of NO_3–N from their application

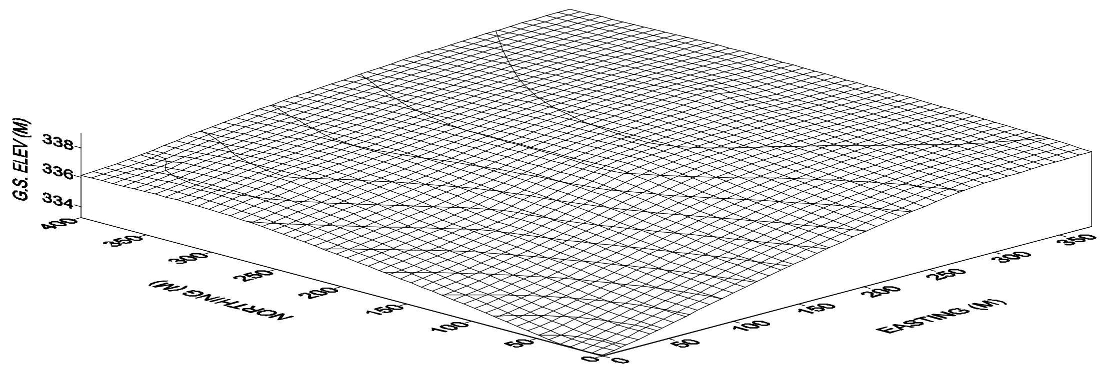

(a)

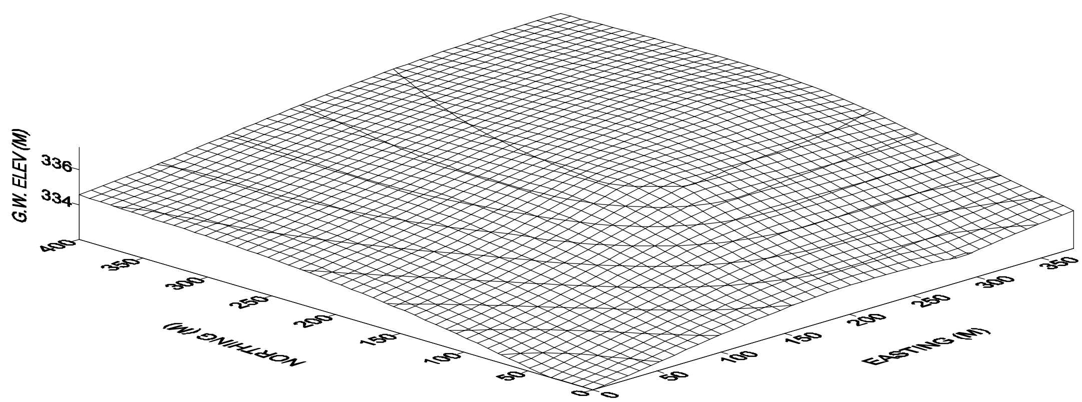

(b)

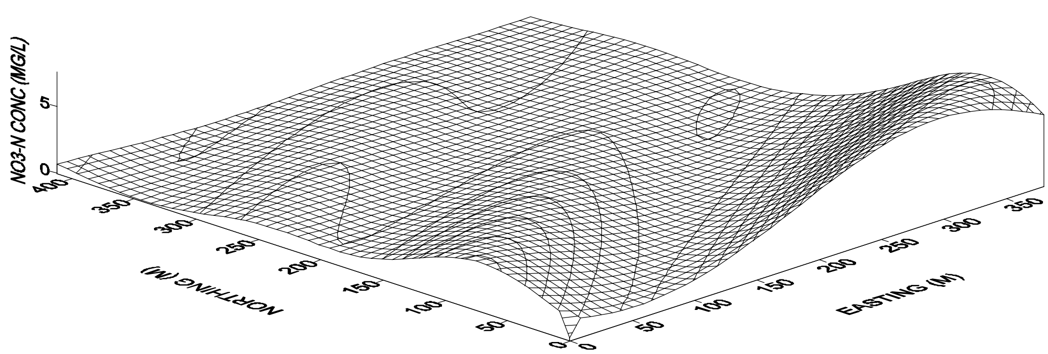

(c)

Figure 9. a) Topographic surface, b) groundwater elevation, and c) average NO_3–N concentration in shallow groundwater at the Ames glacial till aquitard.

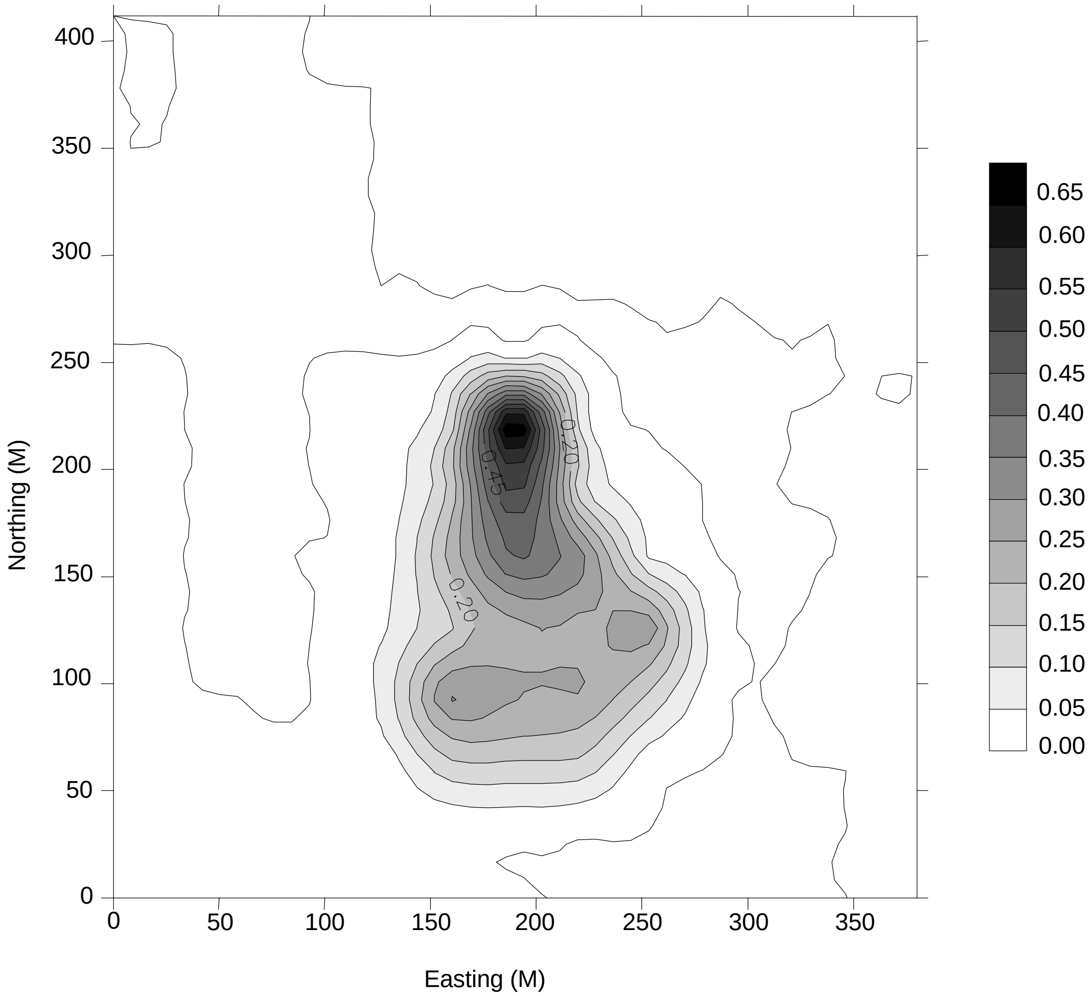

Figure 10. Contour map of backtransformed kriged estimates of NO_3–N concentration in deep groundwater using average observed values (NO_3–N in mg/L).

sources to the low–lying areas is more pronounced for the shallow layers than for the deeper layers.

Geostatistically estimated NO_3–N concentration values based on ordinary kriging proved to be adequate for estimating NO_3–N loading rates in the glacial till aquitard owing to satisfactory cross–validation results of the variogram models used, yielding a mean reduced error of –0.01 to –0.074 and reduced variance of 0.6 to 2.18. Nevertheless, further investigation, particularly for NO_3–N concentration in deep groundwater, using more extensive data sets may substantially improve the results of geostatistical analysis and may lead to more conclusive findings.

Acknowledgements

The authors wish to acknowledge Carl Pederson of the Agricultural and Biosystems Engineering Department, Iowa State University, for his help with groundwater sampling and site map preparation, and Amy Morrow and Diane Farris of the National Soil Tilth Laboratory, USDA, for their help in performing the laboratory analysis.

References

Clark, I. 1979. *Practical Geostatistics*. London, U.K.: Applied Science Publishers, Ltd.

Englund, E., and A. Sparks. 1991. *Geostatistical Environmental Assessment Software (GEO–EAS 1.2.1) User's Guide*. Las Vegas, Nevada: Environmental Monitoring Systems Laboratory, Office of Research and Development, U.S. EPA.

Espinosa, R. J., L. M. Sanchez, A. P. Bosch, and F. Navarrete. 1996. Geostatistical study of nitrate contents in the aquifers of Campo de Dalias (SE Spain). In *GeoEnv I: Geostatistics for Environmental Applications*, 139–151. A. Soares, J. G. Hernandez, and R. Froidevaux, eds. Dordrecht, the Netherlands: Kluwer Academic Publishers.

Gambolati, G., and G. Volpi. 1979. Groundwater contour mapping in Venice by stochastic interpolators: 1. Theory. *Water Resources Research* 15(2): 281–290.

Goderya, F. S., M. F. Dahab, W. E. Woldt, and I. Bogardi. 1996. Spatial patterns analysis of field soil nitrate. In *Geostatistics for Environmental and Geotechnical Applications*, 248–261. S. R. Rouhani, R.M. Srivastava, A. J. Desbarats, M. V. Cromer, and A. I. Johnson, eds. West Conshohocken, Pennsylvania: American Society for Testing and Materials.

Isaaks, E. H., and R. M. Srivastava. 1989. *Applied Geostatistics*. New York, N.Y.: Oxford University Press.

Journel, A. G., and C. J. Huijbregts. 1978. *Mining Geostatistics*. New York, N.Y.: Academic Press.

Kanwar, R. S., J. L. Baker, R. Horton, R. L. Handy, L. C. Jones, and W. W. Simpkins. 1993. *Aquitard Hydrology Project Annual Progress Report*. Ames, Iowa: Department of Agricultural and Biosystems Engineering, Civil and Construction Engineering and Agronomy, Iowa State University.

Kitanidis, P. K. 1997. *Introduction to Geostatistics*, Cambridge University Press. 249 pp.

Marquardt, D.W. 1963. An algorithm for least squares estimation of non–linear parameters. *J. Soc. Ind. Appl. Math*. 11: 431–441.

Rouhani, S. R., R. M. Srivastava, A. J. Desbarats, M. V. Cromer, and A. I. Johnson. 1996. *Geostatistics for Environmental and Geostatistical Applications*. West Conshohocken, Pennsylvania: American Society for Testing and Materials.

Yates, S. R., and M. V. Yates. 1990. *Geostatistics for Waste Management: User's Manual for the GEOPACK*. Version 1.0. Ada, Oklahoma: Robert S. Kerr Environmental Research Laboratory, Office of Research and Development, U.S. EPA.